

Thomson Scattering Measurements of Saturated Ion Waves in Laser Fusion Plasmas

S. H. Glenzer,¹ L. M. Divol,² R. L. Berger,¹ C. Geddes,¹ R. K. Kirkwood,¹
J. D. Moody,¹ E. A. Williams,¹ and P. E. Young¹

¹L-447, Lawrence Livermore National Laboratory, University of California, P.O. Box 808, Livermore, California 94551

²CEA/DIF/DCSA/SET, BP 12, 91680 Bruyères-Le-Châtel, France

(Received 20 October 2000)

We have measured the characteristics of saturated ion-acoustic waves in inertial confinement fusion plasmas. A 263-nm probe laser has been applied to simultaneous Thomson scatter on both ion-acoustic waves excited by thermal electrostatic fluctuations and by stimulated Brillouin scattering of a kilojoule laser beam of varying intensity. The Thomson scattering spectra show saturated ion-wave amplitudes for intensities above $5 \times 10^{14} \text{ W cm}^{-2}$ consistent with three dimensional nonlinear wave modeling.

DOI: 10.1103/PhysRevLett.86.2565

PACS numbers: 52.35.Fp, 52.25.Os, 52.38.-r, 52.70.Kz

The stimulated Brillouin scattering (SBS) instability results from the parametric coupling of an intense incident light wave with an ion-acoustic wave to produce a reflected light wave. SBS can, in principle, reflect a large fraction of the incident energy (up to 100% reflectivity has been observed [1]) and therefore can have a large effect on the coupling of laser energy into targets. As one increases the incident laser energy above the SBS instability threshold, the growth of the SBS instability initially has an exponential dependence on laser intensity, but this growth is expected to saturate. Studying SBS saturation in hot, dense plasmas is important to understand the underlying physics of laser-plasma interactions and to extrapolate scattered light levels from current experiments to the plasma conditions expected in inertial confinement fusion (ICF) targets.

Early Thomson scattering (TS) experiments [2–7] studied saturated ion-wave fluctuations driven by the SBS instability [8] of long-wavelength CO₂ lasers in cold, low-density plasmas. It has been shown that the threshold for the onset of saturation was consistent with the onset of nonlinear damping of the ion-acoustic waves by ion trapping. This effect was found to be important in early simulations [9], and is presently also observed in particle-in-cell (PIC) simulations for ICF plasma conditions [10]. The simulations indicate that trapping flattens the ion velocity distribution function at the ion sound speed and further induces fluctuations of the ion sound speed itself due to the bouncing of the trapped ions. While the former effect reduces linear Landau damping of the ion-acoustic wave, the latter induces a frequency and \mathbf{k} -vector mismatch for the parametric SBS instability saturating the ion-wave amplitude by mitigating SBS [11]. However, recent PIC simulations have further indicated that a frequency mismatch is followed by the decay of large amplitude ion-acoustic waves into two daughter ion waves [12]. This nonlinear saturation mechanism directly limits the amplitude of the ion-acoustic waves. Such a saturation model is presently being applied to simulate SBS measurements from ICF hohlraums [13]. Although these types of simulations indicate the importance of including

nonlinear damping and saturation into the modeling, there has up to now been no direct measurements of saturated SBS ion waves for conditions of interest to ICF [13,14].

In this Letter, we present the first measurements of saturated ion acoustic wave amplitudes in laser plasmas similar to those anticipated in future ignition experiments. For these measurements, we have applied ultraviolet TS of a 263-nm probe beam [15] in well-characterized large scale-length gas bag plasmas with an electron temperature of $T_e = 3 \text{ keV}$. The temporally resolved TS spectra show simultaneously the scattering from thermal electrostatic fluctuations and ion-acoustic waves that have been excited to large amplitudes by SBS from a kilojoule interaction beam at 351 nm. By varying the intensity, I , of the interaction beam, we observe that the ion-acoustic waves saturate for $I > 5 \times 10^{14} \text{ W cm}^{-2}$. These results of the *local* TS measurements are also consistent with the observed SBS reflectivity that shows saturation at the 30% level for these interaction beam intensities.

The comparison with calculations using the laser-plasma interaction code PF3D [16], in which the incident laser and reflected light drive ion-acoustic waves by ponderomotive forces that backscatter, self-focus, and forward-Brillouin scatter the light, indicates that the saturation is consistent with $\delta n/n_e = 2 \times 10^{-3}$. Because this ion-wave fluctuation level (normalized to the electron density, n_e) is appreciably smaller than the threshold for ion trapping, i.e., $\delta n/n_e \sim 0.2$ for our conditions, a simplified nonlinear damping model has been implemented based on the secondary decay of ion-acoustic waves [12]. We find that both reflectivity and TS data can be reproduced with this saturation model.

The experiments were performed at the Nova Laser Facility at the Lawrence Livermore National Laboratory [17]. Nearly spherical gas bags [Fig. 1(a)] of ~ 2.5 -mm diameter have been heated with nine 1-ns-long frequency-tripled (3ω) laser beams. The gas bags [14,18] have been filled with 1 atm of CO₂ plus 1% Ar ($n_e = 6 \times 10^{20} \text{ cm}^{-3}$) to approximate the low ion-wave damping that occurs in the high- Z wall plasma of an ICF hohlraum, where

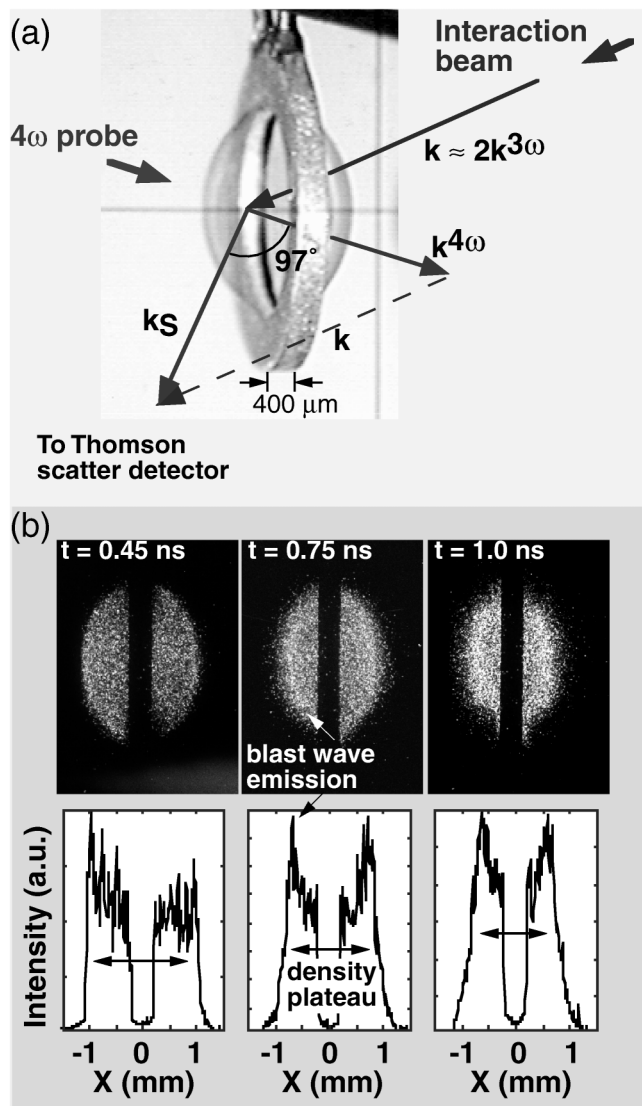


FIG. 1. (a) Gas bag target with \mathbf{k} -vector matching condition for scattering of the probe beam from ion waves that are driven by the interaction beam. (b) The x-ray emission, as a function of time, during the heating of the plasma together with lineouts.

experiments and calculations have shown large gain values for SBS [13]. Nine $f/4.3$ beams delivered a total energy of 21 kJ in a 1-ns square pulse heating the gas bag plasma homogeneously to an electron temperature of $T_e = 3$ keV as measured with 90° TS.

The interaction beam (a 1-ns-long 3ω beam) has been delayed by 0.5 ns with respect to the nine heater beams. It was focused into the gas bag plasma with a random phase plate (RPP) to drive ion waves to large amplitudes in the direction of the laser. The averaged vacuum intensity of the interaction beam was in the range of $3 \times 10^{13} < I < 8 \times 10^{15} \text{ W cm}^{-2}$. We investigate the ion waves with spectrally and temporally resolved measurements of the Thomson scattered 4ω probe light and of the total backreflected laser light from the interaction beam.

Figure 1(a) shows a gas bag target before it has been pressurized together with a schematic of the laser beams

and \mathbf{k} vectors involved in the TS experiment. We have employed a 50-J 4ω probe laser [15] ($\lambda_0 = 263.3$ nm) which is essential for this study because it allows us to match the TS \mathbf{k} vector, $|k| = 2k^{4\omega} \sin(\theta/2)$, $k^{4\omega} = 2\pi/263.3$ nm, with the \mathbf{k} vector of the ion wave driven by SBS from the 3ω interaction beam, $|k| = 2k^{3\omega}$, $k^{3\omega} = 2\pi/351.1$ nm. For this purpose we have observed the TS light at an angle of $\theta = 97^\circ$ to the 4ω laser using a periscope and a Cassegrain telescope. We have applied $f/10$ optics to image the cylindrical scattering volume of $\sim 100 \mu\text{m}$ length and a diameter of $\sim 80 \mu\text{m}$ onto the entrance slit of a 1-m spectrometer. An optical S-20 streak camera has been employed, giving TS spectra with a wavelength resolution of 0.1 nm and a temporal resolution of 100 ps.

The TS volume has been chosen to be at a radial distance of $800 \mu\text{m}$ from the gas bag center. Measurements of the transmitted and backscattered laser power indicate that the interaction beam power at the scattering volume is at least 60% of the initial power. At $t = 0.8$ ns, we find with standard 90° TS [15] that gradients are small, $\Delta T_e/T_e = 10\%$, $\Delta V/C_s \leq 5\%$, where V is the flow velocity and C_s is the sound speed. Two-dimensional x-ray images [Fig. 1(b)] which measure the gas bag emission with energies $E < 2$ keV with a temporal resolution of 80 ps further show a homogeneous emission for $t > 0.3$ ns, indicating that the gas bags are homogeneously heated [13]. At the edges of the gas bag plasma the images show weakly enhanced emission (so-called limb brightening) that is associated with a blast wave which moves towards the gas bag center with the sound speed. The horizontal lineouts show that the blast wave passes through the TS volume at $x = 0.8$ mm at $t \approx 1$ ns.

Figure 2 shows a streak camera record of the temporally resolved TS spectrum from ion-acoustic wave fluctuations with wave number $\mathbf{k} = 2\mathbf{k}^{3\omega}$ along with two lineouts. For this measurement, the 4ω probe laser has been on for $0.5 < t < 1.5$ ns coinciding with the duration of the 3ω interaction beam, the latter with an intensity of $2 \times 10^{15} \text{ W cm}^{-2}$. Weak broadband background radiation can be identified for the duration of the heater beams, i.e., $0 < t < 1$ ns. For $0.5 < t < 1.5$ ns, we observe three different regimes of TS, one of which is due to the arrival of the blast wave at $t = 1$ ns and which separates the coherent and incoherent scatterings.

First, for $0.5 < t < 1$ ns, the spectrum is asymmetric and is dominated by the blueshifted ion-acoustic wave. It is due to coherent scattering [19] off an ion-acoustic wave which is excited to large amplitudes by SBS from the 3ω interaction beam. The redshifted feature can be identified on the streak image at 263.7 nm and is due to scattering off thermal electrostatic fluctuations, resulting in 2 orders of magnitude smaller intensity.

In the second scattering regime, at $1.0 < t < 1.1$ ns, we observe a sudden enhancement of the thermal feature and a wavelength shift of the whole TS spectrum to the red by the ion sound speed. Since this observation coincides with the expected presence and speed of the blast wave [Fig. 1(b)],

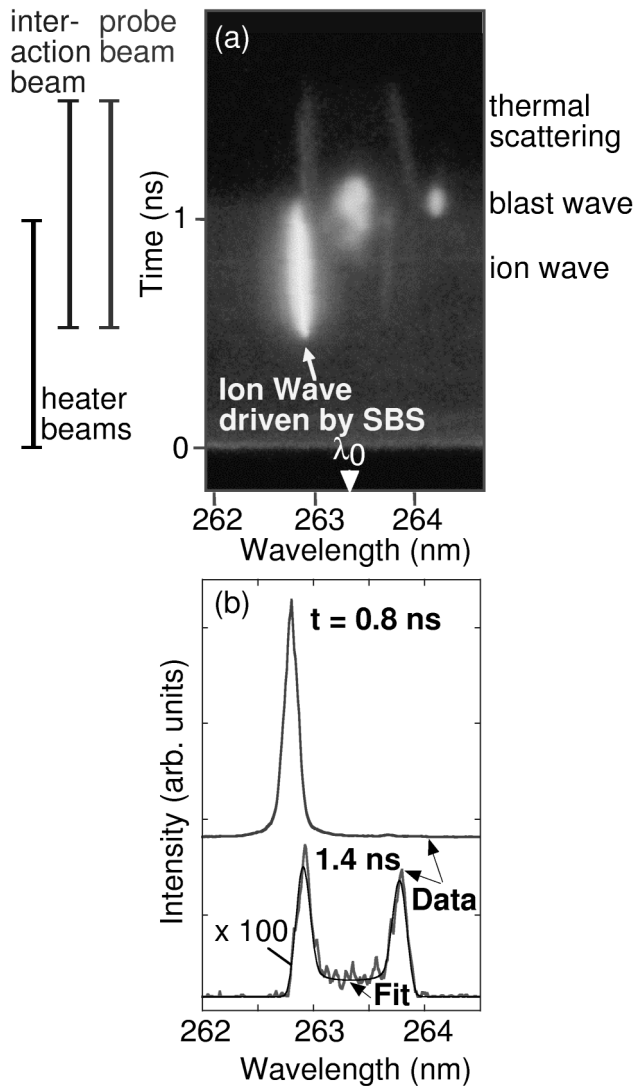


FIG. 2. (a) Time-resolved Thomson scattering spectrum showing coherent scattering on ion waves driven by SBS, scattering on the blast wave, and thermal incoherent scattering at late times. The time sequence of the laser beams is indicated on the left. (b) Lineouts at $t = 0.8$ ns and $t = 1.4$ ns. The earlier lineout shows 2 orders of magnitude enhanced scattering compared to the spectrum at later times. The latter is fit with the theoretical TS form factor for a gas fill of CO₂ plus 1% Ar.

we assume that this shifted burst of the scattering signal is due to enhanced ion-acoustic fluctuations in the blast wave [20]. We note that these enhanced fluctuations are strictly in the radial direction parallel to the velocity of the blast wave and are not associated with a significantly enhanced electron density. The standard 90° TS which probes ion-acoustic wave fluctuations in a different direction does not show these enhanced scattering features.

Finally, for $1.1 < t < 1.5$ ns, when the blast wave has passed through the scattering volume, we measure a standard, fairly symmetric, incoherent TS spectrum with two ion-acoustic peaks for wave fluctuations copropagating and counterpropagating along the scattering vector \mathbf{k} . The whole scattering spectrum is slightly redshifted due to

macroscopic plasma motion. For these times there is no enhancement of the blueshifted ion-acoustic peak due to SBS although the 3ω interaction beam is still on and the instantaneous SBS reflectivity is still high. However, outside of the blast wave the velocity gradients are large enough ($\Delta V/C_s > 15\%$ from the redshift of the TS spectrum) to stabilize the SBS interaction locally confirming that hydrodynamic waves can produce density and velocity gradients, preventing the growth of ion waves to large amplitudes [18,21].

Figure 3(a) shows the intensity ratio of the enhanced blue coherent scattering amplitude to the intensity of the thermal red incoherent component for various 3ω interaction beam intensities. The amplitude of the red component at $t = 0.8$ ns has been assumed to be thermal because its amplitude is approximately the same as for $t = 1.4$ ns, when the whole spectrum can be fitted with the theoretical TS form factor [15]. The parameters for the fit are $T_e = 2.5$ keV and $T_i = 1.7$ keV, in agreement with hydrodynamic simulations. For 3ω interaction beam intensities of $I = 3 \times 10^{13}$ W cm⁻², we find that the ratio in

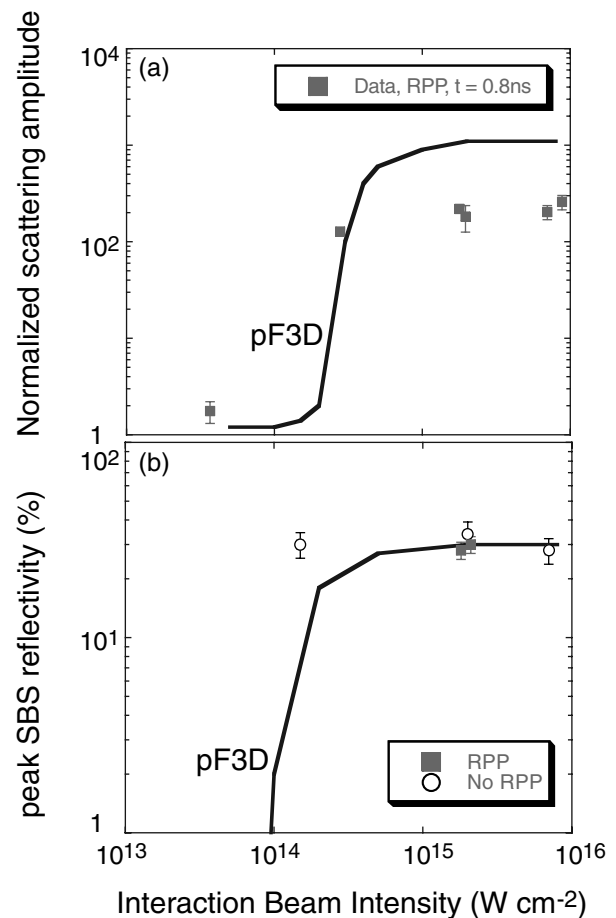


FIG. 3. (a) Scattering amplitude of the blueshifted ion-acoustic wave normalized to the intensity of the redshifted thermal peak for various interaction beam intensities. Amplitudes are for $t = 0.8$ ns. (b) SBS reflectivity for no RPP data is observed to saturate at the 30% level. In both (a) and (b), the PF3D curves represent modeling.

Fig. 3(a) is 1.8 and the blue ion-wave amplitude is close to thermal.

For larger intensities, the ion-wave amplitude grows due to the SBS instability and saturates for vacuum laser intensities of $I > 5 \times 10^{14} \text{ W cm}^{-2}$. Measurements of the SBS reflectivity at $t = 0.8 \text{ ns}$ show no increase for $I > 2 \times 10^{14} \text{ W cm}^{-2}$ [cf. Fig. 3(b)] consistent with saturation. SBS spectra (see also Ref. [18]) are consistent with the TS measurements showing a narrow feature ($\Delta\lambda = 0.25 \text{ nm}$), that is redshifted by 0.8 nm from the incident wavelength, indicating a stationary plasma at $T_e = 3 \text{ keV}$. Since the TS spectra shown in Fig. 2 are also taken from an almost stationary plasma we conclude that the saturation of the ion-wave amplitude shown in Fig. 3(a) limits the SBS reflectivity.

The experimental results are compared to PF3D modeling (see Fig. 3). Nonlinear saturation processes are not self-consistently included in the PF3D code. The ion-acoustic wave amplitude has been limited at a level that scales with the threshold for two-ion-wave decay. By simulating the propagation and SBS scattering of the 3ω interaction beam through the whole length of the gas bag plasma, we find that 30% SBS corresponds to an ion-wave amplitude of $\delta n/n_e = 2 \times 10^{-3}$. Without nonlinear damping, the simulations show 100% reflectivity and ion-acoustic fluctuations in the TS volume that return to the thermal level after a short initial burst, both in contradiction with experimental data. The width of the saturated blueshifted ion-acoustic resonance [Fig. 2(b)] at $t = 0.8 \text{ ns}$ is found to be the same as for the thermal TS spectrum at $t = 1.4 \text{ ns}$, i.e., $\Delta\lambda = 0.17 \text{ nm}$. This width gives an upper bound for a possible frequency mismatch due to ion trapping, plasma-induced bandwidth, or increased damping (e.g., Refs. [22–24]). Localized heating of the plasma with increasing 3ω interaction beam intensity can be ruled out because the TS spectra observe both the blueshifted and the redshifted ion-acoustic peak, giving no measurable temperature increase for $t < 1 \text{ ns}$.

The saturation level is further tested by postprocessing the PF3D simulations estimating the TS power from ion waves driven by the RPP-smoothed interaction beam. The comparison with the experimental data in Fig. 3(a) shows that the onset of enhanced TS around $4 \times 10^{14} \text{ W cm}^{-2}$ is well reproduced, and the calculated scattering off saturated acoustic waves is of the same order of magnitude as seen in the experiments.

The amplitude of the TS is proportional to $(\delta n/n_e)^2 L_c$, where L_c is the correlation length along the direction of the collecting optics. L_c can be approximated by the diameter of the $f/4$ interaction beam speckles. The PF3D code gives a similar result for transverse correlation lengths, which provides an estimate for the angular spray of the scattered light and is consistent with the absence of an enhanced signal at 90° . The remaining small discrepancy with the nonlinear model might be explained by the uncertainty

in the absolute measured scattering power introduced by the Cassegrain telescope (alignment and incomplete sampling). The saturation modeling in PF3D implies no additional nonlinear frequency mismatch or shift (which is consistent with the TS spectrum) so that the three waves participating in the SBS process keep their phase matching over the gas bag's density plateau of $\sim 2 \text{ mm}$. Therefore, the SBS reflectivity is predicted to scale with the square of the full length of the gas bag density plateau [Fig. 1(b)], in agreement with the experimental SBS time history.

In summary, we have shown with ultraviolet TS that ion-acoustic waves saturate in inertial confinement fusion plasmas. The experiments have been performed in a well-characterized gas bag plasma allowing comparisons with simulations. Modeling, using the code PF3D, has reproduced the experimental threshold and saturation behavior for SBS. Our findings indicate that laser scattering losses in future ignition experiments might be reduced by controlling the plasma conditions together with the nonlinear wave saturation processes.

We thank B. J. MacGowan, W. Rozmus, and D. S. Montgomery for helpful discussions. This work was performed under the auspices of the U.S. Department of Energy by University of California, Lawrence Livermore National Laboratory under Contract No. W-7405-Eng-48.

-
- [1] J. Handke *et al.*, Appl. Phys. **25**, 109 (1981).
 - [2] A. Ng *et al.*, Phys. Rev. Lett. **42**, 307 (1979).
 - [3] M. J. Herbst *et al.*, Phys. Rev. Lett. **43**, 1591 (1979).
 - [4] C. E. Clayton *et al.*, Phys. Rev. Lett. **51**, 1656 (1983).
 - [5] B. Gellert and B. Kronast, Appl. Phys. B **32**, 175 (1983); *ibid.* **33**, 29 (1984).
 - [6] J. E. Bernard and J. Meyer, Phys. Rev. Lett. **55**, 79 (1985); Phys. Fluids **29**, 2313 (1986).
 - [7] C. J. Walsh and H. A. Baldis, Phys. Rev. Lett. **48**, 1483 (1982).
 - [8] W. L. Kruer, *The Physics of Laser Plasma Interactions* (Addison-Wesley, New York, 1988).
 - [9] D. W. Forslund *et al.*, Phys. Fluids **18**, 1017 (1975).
 - [10] K. Y. Sanbonmatsu *et al.*, Phys. Rev. Lett. **82**, 932 (1999).
 - [11] J. Handke *et al.*, Phys. Rev. Lett. **51**, 1660 (1983).
 - [12] B. I. Cohen *et al.*, Phys. Plasmas **4**, 956 (1997).
 - [13] S. H. Glenzer *et al.*, Phys. Plasmas (to be published); S. H. Glenzer *et al.*, Phys. Rev. E **55**, 927 (1997).
 - [14] J. D. Lindl, Phys. Plasmas **2**, 3933 (1995).
 - [15] S. H. Glenzer *et al.*, Phys. Plasmas **6**, 2117 (1999).
 - [16] R. L. Berger *et al.*, Phys. Plasmas **5**, 4337 (1998); C. H. Still *et al.*, Phys. Plasmas **7**, 2023 (2000).
 - [17] E. M. Campbell *et al.*, Laser Part. Beams **9**, 209 (1991).
 - [18] D. S. Montgomery *et al.*, Phys. Plasmas **5**, 1973 (1998).
 - [19] R. E. Slusher and C. M. Surko, Phys. Fluids **23**, 472 (1980).
 - [20] J. W. Paul *et al.*, Nature (London) **223**, 822 (1969).
 - [21] A. V. Maximov *et al.*, Phys. Plasmas **3**, 1689 (1996).
 - [22] M. V. Medvedev *et al.*, Phys. Rev. Lett. **81**, 5824 (1998).
 - [23] W. Rozmus *et al.*, Phys. Fluids B **4**, 576 (1992).
 - [24] J. A. Heikkinen *et al.*, Phys. Fluids **27**, 707 (1984).